Available online at www.sciencedirect.com

SciVerse ScienceDirect

Ceramics International 38 (2012) 1463–1471

CERAMICS INTERNATIONAL

www.elsevier.com/locate/ceramint

Environment-dependent indentation recovery of select soda-lime silicate glasses

Mirabbos Hojamberdiev *, Harrie J. Stevens, William C. LaCourse

Kazuo Inamori School of Engineering, Alfred University, Alfred, NY 14802, United States

Received 3 August 2011; accepted 12 September 2011
Available online 17 September 2011

Abstract

Indentations made on silicate glasses can easily be affected by the environment. In the present work, indentations were made on select commercial float glasses as well as on experimental soda-lime silicate glasses using a 1 mm diameter spherical tungsten carbide ball-mounted Brinell indenter. Recovery of indentations made on the glass samples was measured in different environments, namely, 100 °C, room temperature/room humidity and 100% relative humidity, as a function of time by using a Zygo laser non-contact profiliometer. Elastic (Young's modulus, bulk modulus, shear modulus and Poisson's ratio) and indentation (Vickers hardness, fracture toughness, brittleness and fracture surface energy) properties of the glasses were also determined by a pulse-echo and Vickers indentation methods, respectively, to correlate with the recovery of indentations. The elastic properties and Vickers hardness are directly proportional to the packing ions present in the glass structure and the strength of an individual bond, whereas the brittleness and fracture toughness more likely depend on molar volume of the glasses. According to the applied environment, a recovery rate of indentations follows the order: room temperature/room humidity <100% relative humidity <100 °C, regardless of glass composition. The reason for higher recovery rate of indentations is attributed to the structural relaxation, which is promoted by a thermodynamic driving force at 100 °C, and stored strain energy in deformation zone, allowing the indentations to regain their original configurations at certain points.

Keywords: C. Mechanical properties; C. Indentation; D. Glass; E. Structural applications

1. Introduction

It is known that silicate glasses normally obey Hooke's law and present an elastic behavior up to failure. When high compression and shear stress are both present, failure can be inhibited and a permanent deformation can occur [1]. In general, the permanent deformation can be represented by either shear flow or densification according to the glass type; for instance, in normal glasses it appears as a shear flow (faulting), and conversely, in anomalous glasses as a densification due to the compaction of an open structure of the silica network [2,3]. Nevertheless, above a critical load, median-radial cracks propagate in normal glasses whilst cone cracks form in anomalous glasses under Vickers indentation. In most cases, loading a glass with a sharp indenter under high compression ultimately leads to the permanent deformation that may chiefly hinder an elastic restoration at low temperature. Hence, Brinell indentation would be advantageous when investigating an environment-dependent recovery of indentations made on glasses without a large fraction of the permanent deformation as well as cracks. However, the recovery rate of delayed elasticity of the glass is associated with a number of parameters, including temperature, atmosphere, humidity, pressure, load, loading time, indenter type, etc.

A time-dependent deformation is characteristic of viscoelastic materials, of which a mechanical analog is Voigt–Kelvin element that displays a recoverable delayed elasticity [4]. Radok [5] suggested a simple approach to time-dependent viscoelastic indentation, when a rigid spherical indenter is loaded on a viscoelastic body, for finding the viscoelastic solution in cases where the corresponding solution for a purely elastic body is known. Theoretical considerations were also made by Sakai and Shimizu [6] on time-dependent viscoelastic deformation and flow during the penetration by flat-ended,

* Corresponding author at: Materials and Structures Laboratory, Tokyo Institute of Technology, 4259 Nagatsuta, Midori, Yokohama 226-8503, Japan. Tel.: +81 44 945 5323; fax: +81 44 945 5358.
E-mail address: mirabbos_uz@yahoo.com (M. Hojamberdiev).

0272-8842/$36.00
doi:10.1016/j.ceramint.2011.09.029

spherical and conical indenters into glass-forming materials at temperatures near the glass transition. Indeed, self-consistency was experimentally proved through the Berkovich indentation on soda-lime glass at various temperatures [7]. In addition to a two-element (elastic-plastic) mechanical model [8], viscous-elastic-plastic (VEP) model has shown good agreement with nanoindentation data obtained using the Berkovich indenter [9].

Recently, a nanoindentation technique has been popular, particularly using a highly instrumented equipment, in characterizing nano- and micro-scale mechanical properties, e.g. hardness, strength, residual stress, fracture and elastic modulus, and an elastic-plastic response of the near-surface region of brittle materials, including oxide and metallic glasses [10,11]. The analysis is mainly based on the Oliver–Pharr method [12], where the load-displacement curve is used. Most recently, a similar method has also been developed to estimate the contact area in an elastic-plastic indentation and to extract the elastic modulus and hardness of an ultra-thin film bonded to the substrate [13].

Indentations made on silicate glasses can fully or partially be recovered owing to the structural relaxation caused by environmental factors, namely, temperature, humidity, pressure and atmosphere. Because the glass structure can easily be displaced and the original configuration can readily be recovered by supplying sufficient activation energy with heat treatment [14]. For example, Mackenzie [15] showed that more than 99% of the original volume of a hydrostatically densified silica could be recovered after annealing at 1000 °C for 1 h. Yoshida et al. [16] described that more than 65% of Vickers indentation volume was recovered for borate glass by annealing the indentations at $T_g \times 0.9$ K for 2 h. By measuring the indentation volume before and after heat treatment at $T_g \times 0.9$ K for 2 h using atomic force microscopy (AFM), the contribution of indentation-induced densification to total indentation deformation beneath a Vickers indenter was estimated to be 92% for silica glass, 61% for soda-lime silicate glass and 4.6% for bulk metallic glass [17]. Sawasato et al. [18] studied the volume recovery of Vickers indentations made on soda-lime silicate glass as a function of annealing temperature and time and estimated the ratio of volume recovery to be 27% after annealing at $T_g \times 0.6$ K and 71% after annealing at T_g. Besides, they also noted that the elastic recovery of a diagonal length was more limited than the elastic recovery of the depth due to the difference in the density distribution under the indentation impression. Most recently, Yoshida et al. [19] evaluated the indentation-induced densification of soda-lime silicate glass under the diamond indenters with different geometries from the volume recovery of indentations by thermal annealing. They found that with the increase in the inclined face angle, the densification contribution decreased and the shear-flow contribution increased. This significant indenter-geometry dependence of densification in glass could be explained by stress distribution under the indenter.

Since soda-lime silicate glass products are widely used in diverse applications and have a direct contact with various environments, it is therefore of interest to investigate the indentation recovery of these glasses in different environments as a function of time. In this work, physico-mechanical properties and indentation recovery of select commercial float glasses and experimental soda-lime silicate glasses are comparatively investigated at 100 °C, room temperature/room humidity and 100% relative humidity as a function of time. The possible mechanisms for the indentation recovery of these glasses are also discussed.

2. Experimental

Three commercial float glasses (ComGlass) and six experimental (ExpGlass) glasses were employed in this study. Their chemical compositions on molar basis are listed in Table 1. An air side of the commercial float glasses was applied for the indentation due to the presence of chemically different surface on the tin side, which could additionally influence on the mechanical properties during the experiment [20]. Experimental glasses were produced by melting 100 g batches of the given compositions in Pt crucibles. Filled crucibles were inserted into a preheated electric furnace at 1000 °C and melted at 1450 °C for 4 h. Melts were poured on a preheated steel plate, held at their respective annealing temperatures for 1 h and then slowly cooled to room temperature. The glass bars were cut into the 25 mm × 20 mm × 3 mm slices by a Buehler IsoMet low-speed saw using a cutting fluid, and the surfaces of glass slices were thoroughly ground and polished using first 180/320/600/800/1200 SiC grit and then 6/3/1/0.25 μm diamond paste. The polished glass slices were ultrasonically cleaned in acetone and re-annealed at 10 °C above their respective T_g determined by using a STA 409CD differential scanning calorimeter (Netzsch-Gerätebau GmbH, Germany).

The densities of the glass samples were measured using the Archimedes method, with kerosene as the liquid medium. Elastic moduli (Young's modulus, bulk modulus, shear modulus and Poisson's ratio) of the glass samples of known thickness were calculated by measuring their longitudinal and shear wave sound velocities by a pulse-echo method [21] using a TDS420 oscilloscope (Tektronix, USA). Indentation properties (Vickers hardness, fracture toughness, brittleness and fracture surface energy) of the glass samples were measured by a Vickers indentation method using a HMV-2000 Micro Hardness Tester (Shimadzu, Japan) with the load of 200 g applied for 15 s.

The Vickers hardness, H_V, was obtained using $H_V = \frac{2P\sin(\theta/2)}{d^2}$, where P is the applied load, θ is the included angle between the opposite faces of the pyramid and d is the average diagonal of the indentation impression. Brittleness was first defined by Lawn and Marshall [22] in the late 1970s as the ratio of hardness to fracture toughness ($B = H/K$) and later intensively discussed with an indentation technique by Sehgal and Ito [23]. Brittleness of the glass samples was calculated using $B = \left(\frac{1}{0.0056}\right)^{3/2}\left(\frac{C}{a}\right)^{3/2}(P)^{-1/4}$, where B-brittleness, $m^{-1/2}$; C-crack length, m; a-indentation diagonal length, m; P-indentation load, N; the quantity (1/0.0056) has units of $N^{1/6}\,m^{-1/3}$. The indentation fracture toughness, K_C, was calculated

Table 1
Chemical compositions of glass samples (mol%).

Sample	SiO_2	Al_2O_3	Fe_2O_3	CaO	MgO	Na_2O	K_2O	Li_2O
ComGlass1	71.46	0.98	0.05	9.09	4.98	13.18	0.26	–
ComGlass2	71.13	0.86	0.04	8.34	5.70	13.30	0.63	–
ComGlass3	100.0	–	–	–	–	–	–	–
ExpGlass1	73.00	–	–	3.00	7.00	17.0	–	–
ExpGlass2	73.00	–	–	3.00	7.00	13.0	4.00	–
ExpGlass3	73.00	–	–	3.00	7.00	13.0	–	4.00
ExpGlass4	75.00	–	–	10.0	–	15.0	–	–
ExpGlass5	75.00	–	–	10.0	–	7.50	7.50	–
ExpGlass6	75.00	–	–	10.0	–	–	15.0	–

using the equation developed by Anstis et al. [24] $K_C = \psi\left(\frac{E}{H}\right)^{1/2}\left(\frac{P}{c_o^{3/2}}\right)$, where ψ is a material-independent constant (=0.016 for Vickers produced radial cracks), E is Young's modulus, H is Vickers hardness, c_o is the average length of the radial crack. The fracture surface energy, γ, was calculated using $\gamma = \left(\frac{K_{IC}^2(1-\nu^2)}{2E}\right)$, where ν is Poisson's ratio.

Indentation experiments were performed on an Instron 5566 universal hydraulic testing machine (Instron, USA) fitted with a 1 mm diameter spherical tungsten carbide ball-mounted indenter. The indenter was driven at a load rate of 0.015 kN/s with a 15 s dwell time at the maximum load of 0.09 kN, which was further used as an optimum load for indenting glass samples without initiating any significant cracks. Before starting the indentation, a correction was accomplished by measuring a displacement drift. Prior to indentation, all the glass samples were carefully cleaned with acetone one more time and dried with a warm air blower in order to remove any debris/dirt on the surface. Just after indentation the glass samples were separately subjected to three different environments (100 °C, room temperature/room humidity and 100% relative humidity) for 0.25, 1, 6, 12, 24 and 48 h to investigate an environment-dependent indentation recovery as a function of time. The residual indentations in the glass samples were scanned after above-mentioned treatment times using a laser non-contact profilometer (Zygo Corporation, USA). After defining the surface plane, the area scan yielded the maximum depth of the indentation. Based on the depth change of the indentations in different environments, recovery of indentations was evaluated as a function of time.

3. Results and discussion

The chemical composition and physico-mechanical property of a glass have a profound impact on indentation recovery. Therefore, the physico-mechanical properties of commercial float and experimental glass samples were first determined, and the average values are summarized in Table 2. For all the glass samples, a close relationship between density, Vickers hardness and elastic moduli can be noticed. The densities of glass samples differ according to the increase in the concentration of the modifiers and the intermediates with high or low atomic weights in the glasses. Because of the absence of the modifier and the intermediate ions in the silica network, the ComGlass3 sample has the lowest density of 2.20 g/cm^3 among all the samples. Compared to the ComGlass1 and ComGlass2, the ExpGlass1-3 samples with higher magnesium content and lower calcium content have relatively lower densities. The ExpGlass2 has a lower density of 2.447 g/cm^3 compared with that of the ExpGlass1 because relatively large effective radii of the two monovalent alkali metals normally reduce the density and increase the specific volume. In the ExpGlass3, the density further decreases to 2.432 g/cm^3 with a partial replacement of sodium by lithium which is one of the four lightest metals. As is known, the structural contraction caused by the small lithium

Table 2
Physico-mechanical properties of glass samples.

Property	Com Glass1	Com Glass2	Com Glass3	Exp Glass1	Exp Glass2	Exp Glass3	Exp Glass4	Exp Glass5	Exp Glass6
Density, ±0.007 g/cm^3	2.528	2.530	2.200	2.448	2.447	2.432	2.481	2.479	2.466
Young's modulus, ±4.83 GPa	74.04	74.15	71.78	68.68	65.98	75.96	72.38	71.11	62.54
Bulk modulus, ±2.94 GPa	45.67	46.07	36.06	43.58	40.02	44.25	46.16	45.32	41.28
Shear modulus, ±1.68 GPa	30.10	30.10	30.72	27.67	26.99	31.43	29.23	28.71	25.07
Poisson's ratio, ±0.015	0.229	0.231	0.168	0.223	0.210	0.236	0. 247	0.238	0.238
Vickers hardness, ±0.08 GPa	5.31	5.37	–	5.27	5.14	5.48	5.36	5.25	4.82
Brittleness, ±0.170 μm$^{-1/2}$	7.611	7.882	–	7.222	6.743	7.486	7.394	7.279	6.689
Fracture toughness, ±0.018 MPa m$^{1/2}$	0.697	0.682	–	0.729	0.760	0.725	0.724	0.721	0.721
Molar volume, cm^3	23.75	23.73	27.32	24.06	24.60	23.70	24.17	25.16	26.28
Fracture surface energy, J/m^2	3.11	2.97	–	3.68	4.21	3.33	3.40	3.45	3.93

and magnesium ions is not restricted to silicate glasses. Quite similar trends are observed in the ExpGlass4-6 samples with a partial and complete substitution of sodium by potassium. In the absence of magnesium, the densities of the ExpGlass4-6 samples (2.466–2.481 g/cm^3) measured are higher than those of the ExpGlass1-3 samples.

As can be seen in Table 2, the elastic properties and Vickers hardness of glass samples are directly proportional to the packing ions present in the glass structure and the strength of the individual bonds, respectively. Note that the indentation properties for the ComGlass3 (vitreous silica) were not obtained. In the absence of Al_2O_3, the substitution of magnesium for calcium resulted in lower elastic moduli and Vickers hardness in the ExpGlass1 and ExpGlass2 samples compared to those of the ComGlass1-3 and ExpGlass3 samples. Normally, Al_2O_3 eliminates non-bridging oxygens, and hence, enhances the connectivity of glasses. Although the field strength of Mg^{2+} is greater than that of Ca^{2+}, molar volume shows a negligible difference. This indicates that the glass structure is not what would be expected based on the smaller size and higher field strength of Mg^{2+}. In contrast, the ExpGlass3 sample shows the highest elastic modulus (75.96 GPa) and Vickers hardness (5.48 GPa). The stronger field strength of smaller alkali modifier (Li^+) ions to the oxygen ions leads to the formation of stronger bonds as well as to the decrease in the size of the interstices near the non-bridging oxygens in the silica network. So the molar volume decreases and the structure becomes more compact, resulting higher resistance to deformation. On the contrary, when the sodium ions were partially or completely replaced by the potassium ions in the ExpGlass5 and ExpGlass6, respectively, in the absence of magnesium ions, elastic moduli and Vickers hardness were much lower than those of the ExpGlass4 containing only sodium as an alkali modifier. Because the potassium ions are larger than the sodium ions and have lower field strength leading to the formation of weaker K–O bonds in the glass structure that gives higher molar volume. The studies focused on the compositional effects of glass on the elastic properties have also confirmed that the glasses containing cations of high field strength and high coordination number have higher elastic moduli than the glasses containing cations of low field strength and low coordination number [25–27].

As shown in Table 2, brittleness of each glass sample is directly proportional to elastic moduli and Vickers hardness, that is, brittleness increases with the increase in elastic moduli and Vickers hardness. Compared to the ComGlass1-3 samples, brittleness is comparatively lower in the ExpGlass1-6 samples, and the reason for that may be associated with the increase in molar volume of the ExpGlass samples. It has been reported [23] that a higher molar volume implies that the glass structure is more open and deformation precedes easily; a large deformation thus results in the suppression of a median cracking and a lowering of brittleness. Since higher molar volume (27.32 cm^3) of silica glass provides higher brittleness ($\sim$9 $\mu m^{-1/2}$), this concept cannot be applied to all glasses. Kurkjian et al. [28] described that the Si-based glasses with the densities approaching that of silica glass are considered to be anomalous. According to the classification made by Sehgal and Ito [29], our experimental glasses are considered to be in an 'intermediate density case' in which low brittleness is caused by the presence of both densification and plastic flow. So far, the lowest brittleness values have been reported to be 1.2 $\mu m^{-1/2}$ for 100% B_2O_3 sample and 4.7 $\mu m^{-1/2}$ for 76SiO_2-14Li_2O-10 K_2O glass owing to the simultaneous existence of densification and plastic flow [29–31].

In ExpGlass3 sample, the brittleness value notably decreases to 7.486 $\mu m^{-1/2}$ with a partial substitution of calcium and sodium by magnesium and lithium, respectively. This is attributed to an insignificant increase in the openness of the glass structure that resulted from the introduction of the smaller modifier (Li^+) and intermediate (Mg^{2+}) ions into the silica network. In particular, a partial and complete substitution of sodium by potassium decreases the brittleness value up to 6.743 $\mu m^{-1/2}$ in the ExpGlass2 sample and 6.689 $\mu m^{-1/2}$ in the ExpGlass6 sample, respectively. According to the Phillips and Thorpe's rigid percolation theory [32,33], the high values of Young's modulus represent more rigid structure for glass that is more resistant to deformation, and brittleness therefore increases with increasing Young's modulus. Interestingly, the addition of the lithium ions decreases fracture toughness as well as fracture surface energy in the ExpGlass3 in comparison with the ExpGlass1 and ExpGlass2 samples. Generally speaking, the basic glass composition with sodium consists of alkali-rich pathways with isolated silica-rich regions and adding a small amount of lithium may change this structure, i.e., the silica-rich regions become more connected and the alkali-rich pathways become less connected. Probably, this may cause the fracture toughness and fracture surface energy to decrease because the glass becomes more rigid.

The fracture surface energy is the energy required to generate Orowan stress that can break the bond and create two new surfaces due to the fracture. The fracture surface energy is different than the thermodynamic surface energy because it takes into account plastic deformation and chemical reaction at the tip of a propagating crack. The calculated fracture surface energies are consistent with the values of fracture toughness and brittleness of the glass samples. Wiederhorn [34] observed the increase in fracture surface energies of glasses with decreasing temperature and increasing Young's modulus. According to the glass type, the fracture surface energies obtained in nitrogen at 27 °C follow the order: 3.50 J/m^2 for lead-alkali silicate, $<$3.82 J/m^2 for soda-lime silicate, $<$4.42 J/m^2 for vitreous silica, $<$4.51 J/m^2 for borosilicate and 4.63 J/m^2 for alumino-silicate glasses. In that work, it was also mentioned that the fracture surface energy may have been affected by small amounts of plastic deformation generated at the crack tip by the high stress fields. Also, Miyata and Jinno [35] estimated the fracture surface energies for lead borate glasses and found that the fracture surface energy decreased with the addition of 17 wt% PbO, increased till 32 wt% PbO and then decreased again with increasing PbO content. This tendency was clarified in terms of the residual stress in the matrix and dispersed particles due to thermal expansion and elastic modulus mismatches. The calculated fracture surface energies for the

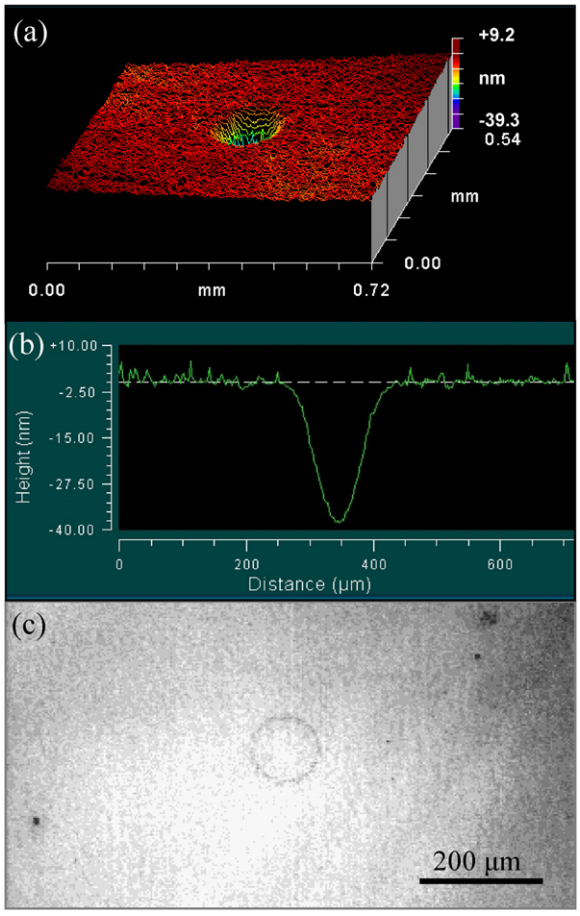

Fig. 1. Landscape (a), trace (b) and optical micrograph (c) of the indentation made on ExpGlass2 sample.

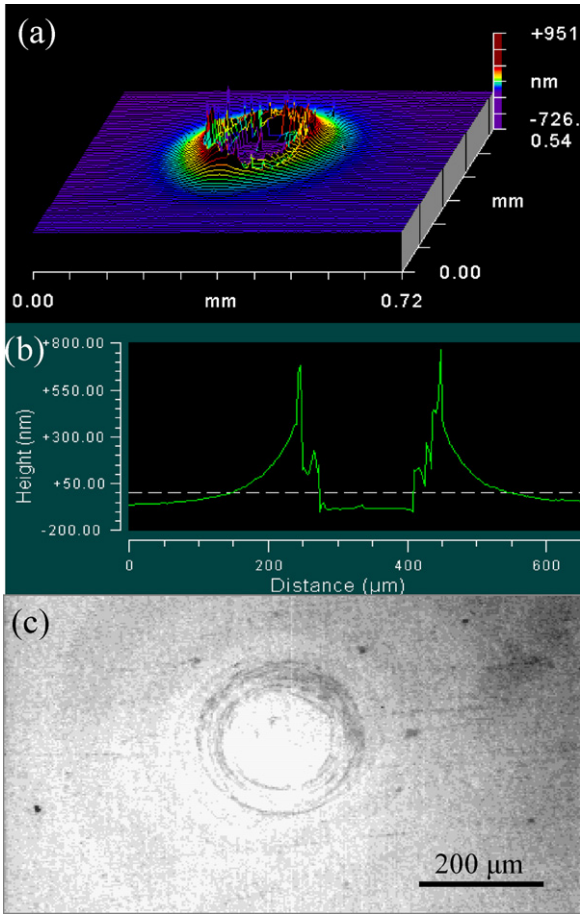

Fig. 2. Landscape (a), trace (b) and optical micrograph (c) of the indentation made on ComGlass3 sample.

ComGlass and ExpGlass samples are in the range of 2.97–4.21 J/m^2. In our case, the fracture surface energies of the glass samples increase as fracture toughness increases but elastic moduli decrease. The increase in fracture surface energy and fracture toughness with the decrease in elastic moduli may have been caused by the 'looser' glass structure that supports less brittleness. This phenomenon was explained by Kennedy et al. [36] as a result of the processes, such as plastic flow, densification and non-recoverable elastic strain energy. Moreover, moisture-containing air can also reduce the force required for the catastrophic failure of glass. According to Shand [37], the lowering of the fracture surface energy is seen to be greater for the high-lead and soda-lime glasses, indicating that these glasses are more sensitive to the presence of water vapor than the other glasses tested.

Fig. 1 represents the landscape, trace and optical micrograph of the indentation made on the ExpGlass2 sample, obtained using a laser non-contact profilometer. Quite surprisingly, almost no material is pushed out to form a pile-up at the rim of the indentation. The analogous behavior was observed by Varshneya et al. [38] for a binary chalcogenide glass with the covalent coordination number of 2.4 and is considered to be as the similarity of a binary chalcogenide glass with 'anomalous' high silica glasses. Generally, the indentations made on anomalous silica glass have sinking-in walls, but not pile-ups, resulted from the reorganization of the silica tetrahedral structural units [SiO_4] by changing the angle of the Si–O–Si bond without breaking it during the loading. Nevertheless, the indentation made on ComGlass3 sample showed a pile-up followed by enormous ring-like cracks with different heights, as shown in Fig. 2. Since the ExpGlass1-6 samples are not anomalous, the reason might be related to the lower stress under the applied load of 0.09 kN and the geometry of the indenter used. Yoshida et al. [19] mentioned that with increasing the inclined face of the indenter, the densification contribution decreases because a large part of glass under the indenter experiences the stress beyond the flow threshold. Howell et al. [39] directly correlated an increasing tendency of four different silicate glasses to pile-up with the decrease in free volume of glass. It was found that a lower value of Poisson's ratio was desired to minimize the pile-up. It has also been shown that the shear-dominated flow will mostly precede compaction in the glass containing a significant fraction of non-bridging oxygen [40]. This shearing along the intermolecular van der Waals forces is easier giving rise to an extensive cracking. It must be noted that above 0.09 kN load a ring-like cracking with different heights around the indentation was observed, and vice versa, below 0.09 kN load the indentations were not detectable for almost all the glass samples. Expectedly, at 0.09 kN load no any significant cracking around the indentation was observed,

as shown in Fig. 1; thereby 0.09 kN was used as the optimum load for the indentation.

As mentioned before, just after the indention all the indented glass samples were immediately subjected to the different environments, namely, 100 °C, room temperature/room humidity and 100% relative humidity, in order to investigate their environment-dependent indentation recovery as a function of time. Apparently, the initial depths of the indentations considerably vary according to their glass compositions and are more likely correlated with the Vickers hardness and elastic modulus. That is, the indentation made on glass possessing

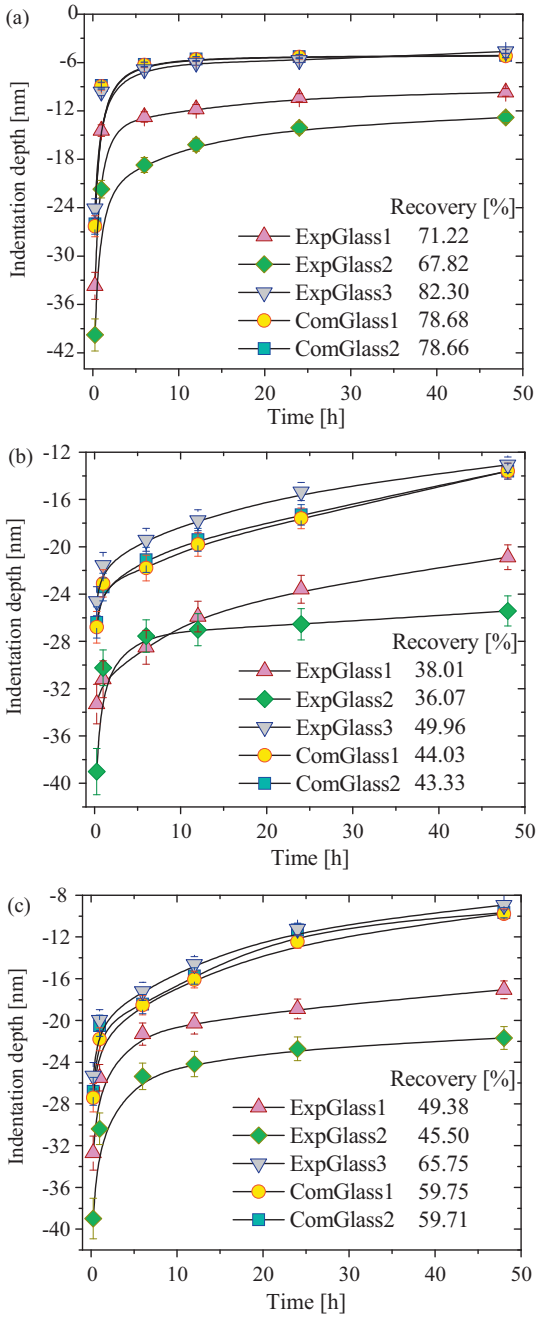

Fig. 3. Change in indentation depth of glass samples (ComGlass1-2 and ExpGlass1-3) at 100 °C (a), room temperature/room humidity (b) and 100% relative humidity (c) as a function of time. Lines drawn as a guide for the eye.

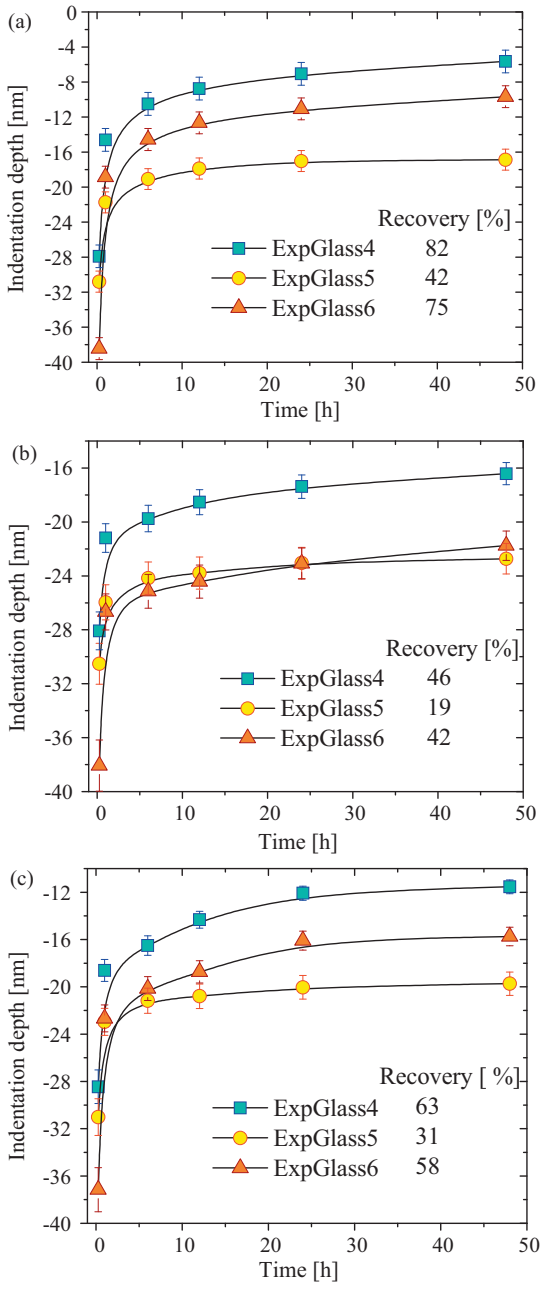

Fig. 4. Change in indentation depth of glass samples (ExpGlass4-6) at 100 °C (a), room temperature/room humidity (b) and 100% relative humidity (c) as a function of time. Lines drawn as a guide for the eye.

higher Vickers hardness is shallow or vice versa due mainly to the rigidity of the glass structure that can resist deformation. As an example, oxygen in the Si–O–K bond in the ExpGlass2 is more strongly deformed compared to those in the other samples as a consequence of the weaker field strength of potassium, and the K^+ ion is more deformable than the Na^+ and Li^+ ions. Owing to their higher field strength, the addition of the Li^+ and Na^+ ions causes much smaller decrease in surface tension.

The indentation recovery of the glass samples at 100 °C, room temperature/room humidity and 100% relative humidity are plotted in Figs. 3–5 as a function of time. According to the applied environment, the recovery of indentations made on

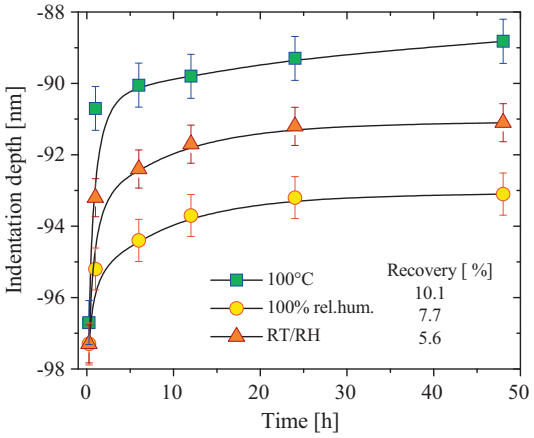

Fig. 5. Change in indentation depth of ComGlass3 sample at 100 °C, room temperature/room humidity and 100% relative humidity as a function of time. Lines drawn as a guide for the eye.

glass samples increases in the following order: room temperature/room humidity <100% relative humidity <100 °C. As shown in Figs. 3a, 4a and 5, heating the indentations made on the glass samples at 100 °C reduced the indentation depths drastically within 6 h compared to those indentations kept at room temperature/room humidity and 100% relative humidity. We also observed that the recovery of indentations with enormous fractures, as shown in Fig. 2a, in the ComGlass3 was not much affected by heating at 100 °C (Fig. 5) due to a large fraction of permanent deformation that might be caused by the bond breakage. As previously reported [41], the indentations made on the lead-phosphate and lead-borate glasses did not show any changes when heated. Glasses with heavy cations usually do not present any thermo-elastic effects, whereas silica glasses with low cation coordination numbers and small Poisson's ratios exhibit strongly.

Environment-dependent indentation recovery rate of the glass samples can be placed as follows: ComGlass3 < ExpGlass5 < ExpGlass2 < ExpGlass1 < ExpGlass6 < ComGlass2 < ComGlass1 < ExpGlass4 < ExpGlass3. Supposedly, a degree of volume instability should be high in the ExpGlass2, ExpGlass3 and ExpGlass5 samples containing mixed alkali ions. The mobility and bond strength of alkali modifier ions in an electrical field take place in the following sequence: K < Na < Li. The kinetics of volume instability (elastic effect and relaxation) is determined by the alkali ion mobility that varies with the size of the second alkali ion, according to its steric requirement (K for Na and Li for Na) and mixed alkali effect [42]. The dissimilar alkali ions are considered to form elastic dipoles which reorient when a mechanical stress is applied. The relaxation time for the reorientation process seems to be determined by the mobility of the less mobile alkali ion because a smaller alkali ion of higher mobility moves first and then a larger alkali ion of lower mobility migrates later. This movement, in turns, generates structural defects. In addition, the thermal pressure caused by thermal movement of atomic particles is completely compensated by internal pressure that approximately coincides with the Vickers hardness of the glass [43].

For those glass samples kept at room temperature/room humidity, the indentation recovery cannot reach equilibrium, as can be seen in Figs. 3b, 4b and 5. Because the indentation recovery at room temperature is low, and therefore it can be greatly facilitated by a thermodynamic driving force at elevated temperature. Most recently, anelastic indentation recovery of bioglass was studied at room temperature [44]. It was experimentally proved that the recovery rate of the indentation depth at room temperature was considered a power-function of the indentation load, i.e. a driving force for the recovery was the stored strain energy over the anelastic indentation zone.

At such a low temperature, the release of internal pressure is not fully enough to support the atoms to regain their original positions completely within the short time range due to the high viscosity although the interatomic separation distance does not exceed the distance corresponding to the maximum restorative force and bonds are not completely broken. In addition to this, the bond bending can also alter the original positions of atoms that may counteract the expansion of the bond length due to the increased amplitude of vibration, resulting in very low thermal expansion coefficients. Filling the interstices inhibits this process and tends to cause an increase in thermal expansion coefficient.

In comparison to the indentation recovery at 100 °C, a slower indentation recovery in 100% relative humidity, as shown in Figs. 3c, 4c and 5, is thought to be due to the structural relaxation caused by a stress-enhanced reaction of water with the glass, as expressed by the following reactions [45]

$$\equiv SiO-O-Na^{+}(K^{+}\text{or}Li^{+}) + H_2O \rightarrow \equiv Si-OH + Na^{+}(K^{+}\text{or}Li^{+}) + OH^{-}$$

$$\equiv SiO-O-Ca^{2+}(Mg^{2+}) + H_2O \rightarrow \equiv Si-OH + Ca$$

$$\equiv Si-O-Si\equiv + OH^{-} \rightarrow \equiv Si-OH + \equiv Si-O^{-}$$

$$\equiv Si-O^{-} + H_2O \rightarrow \equiv Si-OH + OH^{-}.$$

Once the first two reactions occur, the depolymerization takes place continuously and then recombination starts

$$2Si-OH \rightarrow = Si-O-Si = + H_2O.$$

After these processes the glass surface normally becomes softer due to the gelation and surface structural relaxation of the glass. This may be the mechanism for the mechanical fatigue, since the hydrated layer reduces mechanical properties [46,47]. Because the adsorption of water on the glass surface lowers the Si–O–Si bond strength, and once this bond is broken, the product ≡SiO and –O–Si≡ will be highly reactive and combine with water that ultimately hampers viscoelasticity of the indentations at certain point. In this case, the bond lengths of different alkali ions with oxygen also play an important role; for instance, the lithium ions have shorter bond lengths with oxygen and higher nuclear coupling frequencies because the polarizability of OH^{-} should be much stronger than $Si–O^{-}$. Furthermore, the stress gradient is known to produce ionic or atomic motion from the compression side to the tension side. It

is found that the diffusion of water is higher on the tensile side, where the diffusing species are moving against the stress gradient. The diffusion coefficient varies simply because the glass volume changes under stress as the diffusion coefficient changes under hydrostatic pressure [48,49].

The indentations made on the glass samples are found to recover by time within the limited range. The applied environment plays a governing role in controlling the contribution of indentation-induced densification to total indentation deformation as well as recovery rates. The indentation depth (d) starts decreasing rapidly with time (t) just after unloading. The indentation recovery rate can be calculated using $\mathrm{Log}d = -m\log t + K$ [50], where m and K are constants. For all the glass samples, the recovery rate, or slope m, is greater at first 6 h, after which it slows down drastically for longer period, due to the high stress induced by indentation. The indentation recovery rate slows according to the test environment in the following order: 100 °C > 100% relative humidity > room temperature/room humidity. Levengood and Vong [50] studied the influence of the loading time on the recovery rate of an indentation, and it was found that the longer loading time could cause a slow recovery rate due to the localized deformation in the center of the indentation.

The indented glass samples demonstrate three common features: elasticity, viscoelasticity (delayed elasticity) and plasticity (irreversible compaction) under hydrostatic compression. Sawasato et al. [18] observed a very fast initial recovery of the indentation volume within the first 15 min at different thermal treatment temperatures. The initial restoration was not measured in this study. It is assumed that there might have been indeed a restoration in the indentations made on the glass samples within that period resulting from the stretching of interatomic bonds when the indentations were first made because the indentation has a strong ability to recover easily due to the instant spring back of the bonds to normal lengths on the basis of restoring force, particularly under a lower load for a shorter time [49]. Viscoelasticity is based on the gradual expansion of the structure in the direction of the applied stress. This is resulted from the disentangling of structural elements, that is, rings or chains. This is the result of stress induced ion migration along with hydration effects. Moreover, the elastic, viscoelastic and plastic behavior of a glass can also be predicted by a Maxwell model that shows a relationship between instantaneous modulus G_0 and viscosity η under constant stress and the time constant of stress relaxation τ_s at constant strain, $\tau = \eta/G_0$. Oyen and Cook [9] also developed a model incorporating in an obvious way the separate elastic, viscous and plastic components and can be used to predict experimental behavior.

Note that the Brinell indenter with a hemispherical tip did not cause the glass samples to reach a critical Hookean point at 0.09 kN load, so all the indentations showed more elasticity and viscoelasticity than plasticity. The deformation energies for silicate glasses during loading using the Vickers indentation technique were estimated by Suzuki et al. [3] and found to be 139 kJ/mol for total deformation, 96 kJ/mol for elastic deformation and 43 kJ/mol for plastic deformation, which is very close to the activation energy (46–54 kJ/mol) for the recovery of densification in silica glass reported so far. Annealing behaviors of silicate, soda-lime silicate and potassium-lead silicate glasses indicated that the nature of fracture-induced structural change was observed to be densification [51].

4. Conclusions

In summary, physico-mechanical properties and environment-dependent recovery of the indentations made on the select commercial float glasses and experimental soda-lime silicate glasses using a 1 mm diameter spherical tungsten carbide ball-mounted Brinell indenter was investigated. The findings from the present work can be summarized as follows:

(1) The elastic properties and Vickers hardness were directly proportional to the packing ions present in the glass structure and the strength of an individual bond. The brittleness and fracture toughness more likely depend on the molar volume of the glasses.
(2) According to the applied environment, an indentation recovery rate followed the order: room temperature/room humidity < 100% relative humidity < 100 °C, regardless of the glass composition. The reason for higher indentation recovery rate is attributed to the structural relaxation, which is promoted by a thermodynamic driving force at 100 °C, and stored strain energy in deformation zone, allowing the indentations to regain their original configurations at certain points.
(3) The recovery rate of the indentations made on glass samples was high at first 6 h and then slowed for longer period. Because the indentation has a strong ability to recover easily within shorter time due to the instantly spring back of the bonds to normal lengths on the basis of restoring force, which was not disturbed by applied load. The longer recovery time is attributed to a stress-induced ion migration.
(4) Recovery rate of the indentations had a dependence on the concentration of the alkali ions present in the silica network. The mobility of the less mobile alkali ion had effect on the reorientation process of the glass structure after unloading because a smaller alkali ion of higher mobility moved first and then a larger alkali ion of lower mobility migrated later.
(5) Although the applying of different environments, the indented glass samples demonstrated three common features: elasticity, viscoelasticity and plasticity.

Acknowledgements

MH would like to thank the Fulbright Scholar Program for the award of a research scholarship under which the present study was carried out. The authors are thankful to Mr. James E. Thiebaud for the immense technical support.

References

[1] M. Bertoldi, V.M. Sglavo, Soda-borosilicate glass: normal or anomalous behavior under Vickers indentation? J. Non-Cryst. Solids 344 (2004) 51–59.

[2] A. Arora, D.B. Marshall, B.R. Lawn, M.V. Swain, Indentation deformation/fracture of normal and anomalous glasses, J. Non-Cryst. Solids 31 (1979) 415–428.
[3] K. Suzuki, Y. Benino, T. Fujiwara, T. Komatsu, Densification energy during nanoindentation of silica glass, J. Am. Ceram. Soc. 85 (2002) 3102–3104.
[4] A.K. Varshneya, Fundamentals of Inorganic Glasses, Academic Press, Boston, 1994.
[5] J.R.M. Radok, Visco-elastic stress analysis, Q. Appl. Math. 15 (1957) 198–202.
[6] M. Sakai, S. Shimizu, Indentation rheometry for glass-forming materials, J. Non-Cryst. Solids 282 (2001) 236–247.
[7] M. Sakai, S. Shimizu, S. Ito, Viscoelastic indentation of silicate glasses, J. Am. Ceram. Soc. 85 (2002) 1210–1216.
[8] M. Sakai, The Meyer hardness: a measure for plasticity? J. Mater. Res. 14 (1999) 3630–3639.
[9] M.L. Oyen, R.F. Cook, Load-displacement behavior during sharp indentation of viscous-elastic-plastic materials, J. Mater. Res. 18 (2003) 139–150.
[10] A. Shimamoto, K. Tanaka, Y. Akiyma, H. Yoshizaki, Nanoindentation of glass with a tip-truncated Berkovich indenter, Philos. Mag. 74 (1996) 1097–1105.
[11] N. Lonnroth, C.L. Muhlstein, C. Pantano, Y. Yue, Nanoindentation of glass wool fibers, J. Non-Cryst. Solids 354 (2008) 3887–3895.
[12] W.C. Oliver, G.M. Pharr, An improved technique for determining hardness and elastic modulus using load and displacement sensing indentation experiments, J. Mater. Res. 7 (1992) 1564–1583.
[13] H. Li, J.J. Vlassak, Determining the elastic modulus and hardness of an ultra-thin film on a substrate using nanoindentation, J. Mater. Res. 24 (2009) 1114–1126.
[14] G.W. Scherer, Relaxation in Glass and Composites, John Wiley and Sons, New York, 1986.
[15] J.D. Mackenzie, High-pressure effects on oxide glasses: II, Subsequent heat treatment, J. Am. Ceram. Soc. 46 (1963) 470–476.
[16] S. Yoshida, Y. Hayashi, A. Konno, T. Sugiwara, Y. Miura, J. Matsuoka, Indentation induced densification of sodium borate glasses, Eur. J. Glass Sci. Tech. Part B 50 (2009) 63–70.
[17] S. Yoshida, J.-C. Sangleboeuf, T. Rouxel, Quantitative evaluation of indentation-induced densification in glass, J. Mater. Res. 20 (2005) 3404–3412.
[18] H. Sawasato, S. Yoshida, T. Sugawara, Y. Miura, J. Matsuoka, Relaxation behaviors of Vickers indentations in soda-lime glass, J. Ceram. Soc. Jpn. 116 (2008) 864–868.
[19] S. Yoshida, H. Sawasato, T. Sugawara, Y. Miura, J. Matsuoka, Effects of indenter geometry on indentation-induced densification of soda-lime glass, J. Mater. Res. 25 (2010) 2203–2211.
[20] J.A. Howell, J.R. Hellmann, C.L. Muhlstein, Nanomechanical properties of commercial float glass, J. Non-Cryst. Solids 354 (2008) 1891–1899.
[21] J. Krautkramer, H. Krautkramer, Ultrasonic Testing of Materials, fourth ed., Springer-Verlag, Berlin and New York, 1990.
[22] B.R. Lawn, D.B. Marshall, Hardness, toughness, and brittleness: an indentation analysis, J. Am. Ceram. Soc. 62 (1979) 347–350.
[23] J. Sehgal, S. Ito, A new low-brittleness glass in the soda-lime-silica glass family, J. Am. Ceram. Soc. 81 (1998) 2485–2488.
[24] G.R. Anstis, P. Chantikul, B.R. Lawn, D.B. Marshall, A critical evaluation of indentation techniques for measuring fracture toughness: direct crack measurements, J. Am. Ceram. Soc. 64 (1981) 533–538.
[25] E.I. Kozlovskaya, Effect of composition in the elastic properties of glass, in: N.A. Toropov, E.A. Porai-Koshits (Eds.), The Structure of Glass, vol. 2, Consultants Bureau, New York, 1960, pp. 445–450.
[26] Y. Vaills, Y. Luspin, G. Huaret, B. Coté, Elastic properties of sodium magnesium silica and sodium calcium silica glasses by brillouin scattering, Solid State Commun. 87 (1993) 1097–1100.
[27] R.R. Shaw, D.R. Uhlmann, Effect of phase separation on the properties of simple glasses. II. Elastic properties, J. Non-Cryst. Solids 5 (1971) 237–263.
[28] C.R. Kurkjian, J.T. Krause, H.J. McSkimin, P. Andreatch, T.B. Bateman, Pressure dependence of elastic constants and Gruneisen parameters in fused SiO_2, GeO_2, BeF_2 and B_2O_3, in: R.W. Douglas, B. Ellis (Eds.), Amorphous Materials, Wiley, London, 1920, pp. 463–473.
[29] J. Sehgal, S. Ito, Brittleness of glass, J. Non-Cryst. Solids 253 (1999) 126–132.
[30] F.C. Eversteijn, J.M. Stevels, H.I. Waterman, Density, refractive index, and specific refraction of vitreous boron oxide and of sodium borate glasses as functions of composition, method of preparation, and rate of cooling, Phys. Chem. Glass. 1 (1960) 134–136.
[31] E. Vernaz, F. Larche, J. Zarzycki, Fracture toughness-composition relationship in some binary and ternary glass systems, J. Non-Cryst. Solids 37 (1980) 359–365.
[32] J.C. Phillips, Topology of covalent non-crystalline solids. I. Short-range order in chalcogenide alloys, J. Non-Cryst. Solids 34 (1979) 153–181.
[33] M.F. Thorpe, Rigidity percolation in glassy structures, J. Non-Cryst. Solids 76 (1985) 109–116.
[34] S.M. Wiederhorn, Fracture surface energy of glass, J. Am. Ceram. Soc. 52 (1969) 99–105.
[35] N. Miyata, H. Jinno, Fracture toughness and fracture surface energy of lead-borate glasses, J. Mater. Sci. Lett. 1 (1982) 156–158.
[36] C.R. Kennedy, R.C. Bradt, G.E. Rindone, Fracture mechanics of binary sodium silicate glasses, in: R.C. Bradt, D.P.H. Hasselman, F.F. Lange (Eds.), Fracture Mechanics of Ceramics, vol. 2, Plenum Press, New York, 1974.
[37] E.B. Shand, Correlation of strength of glass with fracture flaws of measured size, J. Am. Ceram. Soc. 44 (1961) 451–455.
[38] A.K. Varshneya, D.J. Mauro, B. Rangarajan, B.F. Bowden, Deformation and cracking in Ge-Sb-Se chalcogenide glasses during indentation, J. Am. Ceram. Soc. 90 (2006) 177–183.
[39] J.A. Howell, J.R. Hellmann, C.L. Muhlstein, Correlations between free volume and pile-up behavior in nanoindentation reference glasses, Mater. Lett. 62 (2008) 2140–2142.
[40] A.K. Varshneya, D.J. Mauro, Vickers hardness, indentation toughness, elasticity, plasticity, and brittleness of Ge-Sb-Se chalcogenide glasses, J. Non-Cryst. Solids 353 (2007) 1291–1297.
[41] W. Diehl, R. Schulze, Z. Angew. Phys. 9 (1957) 251.
[42] W.C. LaCourse, A defect model for the mixed alkali affect, J. Non-Cryst. Solids 95-96 (1987) 905–912.
[43] V. Belostotsky, Defect model for the mixed mobile ion effect, J. Non-Cryst. Solids 353 (2007) 1078–1090.
[44] D. Li, F. Yang, Anelastic indentation recovery of bioglass at room temperature, J. Non-Cryst. Solids 356 (2010) 169–171.
[45] R.J. Charles, Static fatigue of glass, J. Appl. Phys. 29 (1958) 1549–1553.
[46] M. Tomozawa, R.W. Hepburn, Surface structural relaxation of silica glass: a possible mechanism of mechanical fatigue, J. Non-Cryst. Solids 345-346 (2004) 449–460.
[47] D.R. Tadjiev, R.J. Hand, Inter-relationships between composition and near surface mechanical properties of silicate glasses, J. Non-Cryst. Solids 354 (2008) 5108–5109.
[48] N. Gougeon, J.-C. Sangleboeuf, R.E. Abdi, M. Poulain, C. Tistere-Borda, Indentation behavior of silica optical fibers aged in hot water, Fiber Integr. Opt. 24 (2005) 491–500.
[49] M. Nogami, M. Tomozawa, Effect of stress on water diffusion in silica glass, J. Am. Ceram. Soc. 67 (2006) 151–154.
[50] W.C. Levengood, T.S. Vong, Observations concerning delayed elastic effects in glass, J. Opt. Soc. Am. 49 (1959) 61–66.
[51] J. Matsuoka, M. Sumita, M. Numaguchi, S. Yoshida, N. Soga, Fracture-induced change in the internal energy of silicate glasses, J. Non-Cryst. Solids 349 (2004) 185–188.